Drag Correlation and Predictions of Surface Groove Drag for Kinetic Energy Projectiles

Ameer G. Mikhail*
U.S. Army Ballistic Research Laboratory, Aberdeen Proving Ground, Maryland

A prediction method for estimating the increment of increase in drag coefficient due to grooves on the surface of the body of a kinetic energy (KE) projectile is established based on wind-tunnel data. Known existing methods give very poor results when compared to experimental data. Twenty cases were considered for the present correlations and validation. The results achieved are very satisfactory. The present analysis considers parameters not included in the existing methods: the groove pitch (or alternately the groove depth); and multigroove types residing on the same projectile body. Groove drag decreases very rapidly with the increase in Reynolds number and also decreases considerably with the increase in Mach number. The range of validity of the present expressions coincides with the usual KE projectile requirement, which establishes the Mach number range to be $3.5 \leqslant M < 5.5$ and $\alpha = 0$ deg.

Nomenclature

A_{ref} = projectile reference area, $(\pi D^2/4)$
C_A = axial force coefficient
C_D = drag coefficient, drag force/$(0.5\rho_\infty V^2 A_{\text{ref}})$
$C_{D_{\text{TSB}}}$ = body-alone total drag coefficient (including base drag) for the smooth body (i.e., without grooves) configuration
$C_{D_{\text{SFSB}}}$ = drag coefficient due to skin friction of the smooth body of the cylindrical portion l_c of the body
c_f = skin-friction coefficient
d_c = diameter of the cylindrical portion, in calibers
D = reference diameter of the projectile
h = groove depth
KE = kinetic energy
l_c = length of the cylindrical portion of the body, in calibers
l_g, l_{g_1}, l_{g_2} = axial length of the grooved portion of the projectile body
L = reference length of the projectile, usually the total length except as otherwise noted
M = projectile Mach number
p = groove pitch
Re = Reynolds number per unit length
Re_L = Reynolds number based on the total length of the projectile
V = projectile velocity
x_o = distance from the nose tip to the first groove
α = angle of attack
ρ_∞ = freestream air density
τ = shear stress at the wall

I. Introduction

THERE are certain types of flight vehicles, namely the kinetic energy (KE) projectiles, which must have relatively large body grooves to hold a sabot that functions as a bore rider inside the gun tube and that separates at a short distance from the muzzle of the gun. These grooves, which usually extend over half of the total length of the projectile, increase the axial force coefficient and therefore the drag. The grooves also affect the aerodynamics of the fins of these projectiles; however, this effect will not be considered in this study.

In recent years, long KE projectiles ($L/D > 20$) have been receiving closer attention due to their terminal ballistics effectiveness. For long penetrators, the groove drag is an increasingly important component of the total drag of the vehicle. It is for this class of projectiles that a method was needed for predicting the increase in the drag coefficient due to these grooves. Reference 1 offers wind-tunnel results for this class of projectiles and represents a basis for validation of the models as well as a basis for a correlation study.

Because the groove drag is small for shorter projectiles ($L/D < 20$) at a Mach number of 5, not many investigations have been carried out for its study. Also, because the effect of grooves on aerodynamics is only of interest to projectile designers, no investigations have been made in the corresponding missile-aerodynamics studies. Therefore, most short KE projectiles are currently designed without any consideration to groove drag. Among the available literature on the subject, Ref. 2 offers an expression for calculating ΔC_{D_g}, without any basis and without any reference to any experimental data for validation. Reference 3 offers a more logically acceptable expression, which is validated using four data points, but is shown to provide much higher values (300% higher) in comparison with the present wind-tunnel data. In addition, Ref. 3 does not disclose the Reynolds number of the wind-tunnel tests.

With only poor prediction capabilities being available, the present work was pursued to fill a void and to provide a prediction capability based on the correlation of the experimental data of Ref. 1 as well as other data provided by Ref. 4. The results of this correlation will be compared to the predictions of both Refs. 2 and 3.

The present correlations include the direct effect of the groove pitch (or the groove depth, since they are directly related for all standard threads). The present analysis also allows for multiple groove types on the same body. An example for this particular projectile configuration is shown in Fig. 1 together with the general nomenclature.

The present work limits itself to zero angle of attack. Therefore, distinction between drag and axial force vanishes and the drag coefficient will be used throughout this report.

Presented as Paper 88-2541 at the AIAA 6th Applied Aerodynamics Conference, Williamsburg, VA, June 6–8, 1988; received June 19, 1988; revision received Feb. 10, 1989. This paper is declared a work of the U.S. Government and is not subject to copyright protection in the United States.

*Aerospace Engineer, Launch and Flight Division.

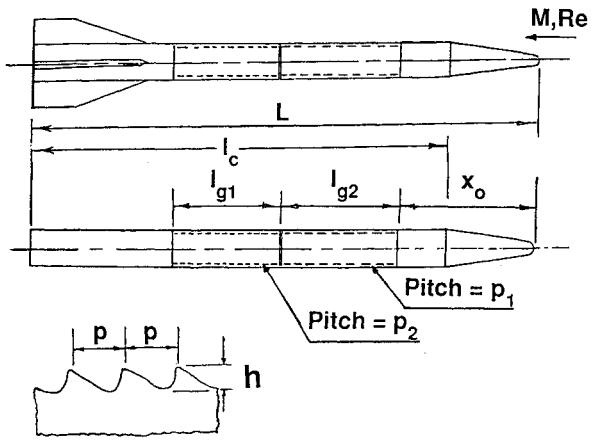

Fig. 1 General configuration and nomenclature for a kinetic energy projectile.

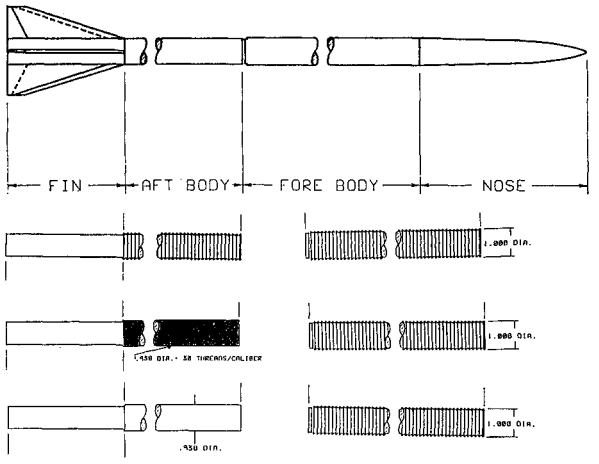

Fig. 2 Wind-tunnel test model for the tests of Ref. 1.

Table 1 Case designation and test conditions of Ref. 1

Case no.	Total length L, caliber	Length and type of threads[a]		Cylindrical length l_c, caliber	Mach number	Re per ft $\times 10^6$	$Re_L + 10^6$ (based on L)
		l_{g1}, caliber	l_{g2}, caliber				
1	20.59	6.366(G)	—	10.417	5.0	5.79	9.32
2	20.59	6.366(G)	4.051(T)	10.417	3.5	4.15	6.68
3	20.59	6.366(G)	4.051(T)	10.417	5.0	5.65	9.09
4	20.59	6.366(G)	4.051(G)	10.417	5.0	5.56	8.94
5	25.59	9.392(G)	—	15.420	5.0	5.68	11.36
6	25.59	9.392(G)	6.028(T)	15.420	3.5	4.19	8.38
7	25.59	9.392(G)	6.028(T)	15.420	4.0	5.23	10.45
8	25.59	9.392(G)	6.028(T)	15.420	5.0	5.41	10.81
9	25.59	9.392(G)	6.028(G)	15.420	5.0	5.88	11.76
10	30.58	12.408(G)	—	20.412	5.0	5.71	13.65
11	30.58	12.408(G)	8.004(T)	20.412	5.0	5.71	13.64
12	30.58	12.408(G)	8.004(G)	20.412	5.0	5.76	13.77
13	35.59	15.424(G)	—	25.420	5.0	5.65	15.72
14	35.59	15.424(G)	9.996(T)	25.420	3.5	3.79	10.55
15	35.59	15.424(G)	9.996(T)	25.420	4.0	4.49	12.48
16	35.59	15.424(G)	9.996(T)	25.420	5.0	5.70	15.83
17	35.59	15.424(G)	9.996(G)	25.420	5.0	5.81	16.15

[a]Type: (G) for grooves (8 grooves per in.). (T) for threads (32 threads per in.).

II. Wind-Tunnel Data and Test

Reference 1 documents tests performed at the supersonic wind tunnel of the Naval Surface Weapons Center Laboratory at White Oak, Maryland. The tests were performed at Mach numbers 3.5, 4.0, and 5.0, with the majority of tests run at $M = 5.0$. The Reynolds number for the tests varied between $4.0-5.8 \times 10^6$ ft^{-1} ($12.2-19.0 \times 10^6$ m^{-1}).

All of the models had a diameter of 0.94 in. (23.9 mm). The models were sting-supported. Four lengths were tested, with L/D of 20.59, 25.59, 30.58, and 35.59. Both body-alone (without fins) smooth-surface and body-alone grooved-surface configurations were tested.

The groovings are made on two body sections, a forward and a rear section. The forward section is always grooved while the rear was either smooth, threaded, or grooved. Grooves are large threads with thick thread profile to carry large loads or to transfer large forces between two bodies. No precise size defines when threads may be denoted as grooves. The notation (G/T) is used to denote grooved forward section and threaded rear section. Figure 2 displays the three basic combinations together with the totally smooth body. Tests were also performed with and without fins; however, the present work excludes the cases with fins in order to obtain a better evaluation of the effects of grooves on the axial force coefficient. The grooves were 8/in. (i.e., pitch = 1/8 in. or 3.17 mm) while the threads were 32/in. (pitch = 1/32 in. or 0.79 mm).

Four different noses were tested, in close resemblance to the 10-deg cone (semivertex angle). They are two Sears–Haack noses and a biconical shape in addition to the 10-deg cone. In the present study, the nose configuration does not affect the results since only the drag increase between smooth and grooved configuration, ΔC_{D_g}, is considered. Most of the tests, however, were run with the Sears–Haack nose. This nose configuration and details of the forward and rear grooves can be found in Refs. 1 and 5.

Examination of the wind-tunnel results of Ref. 1 indicated that the measurements are not always perfect and the accuracy of the result may be affected. For example, the axial force coefficient for some cases did not exhibit symmetry for positive and negative α. Some obvious errors for other cases for the normal force existed, usually for negative α. With such long projectiles being supported by a sting from its base, possible rod bending may partially explain the source of asymmetry with respect to α.

Seventeen test cases were identified from the data of Ref. 1 and they are listed in Table 1. The total pressure of the wind tunnel varied between 2.4–8.2 times the atmospheric value.

A second set of data was obtained from Ref. 4. These data consisted of three tests at Mach numbers 3.49, 3.98, and 4.75

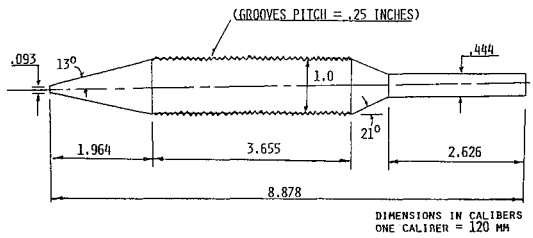

Fig. 3 Wind-tunnel test model for the tests of Ref. 4.

Table 2 Case designation and test conditions of Ref. 4

Case no.	Mach number	Re/ft $\times 10^{-6}$	C_D Wind tunnel, Grooved body	C_D Wind tunnel, Smooth body	ΔC_{D_g} Wind tunnel
18	3.49	12	0.280	0.255	0.025
19	3.98	14	0.227	0.208	0.019
20	4.75	18	0.196	0.186	0.010

with a corresponding tunnel Reynolds number of 12×10^6, 14×10^6, and 18×10^6 ft^{-1} (39.4×10^6, 45.9×10^6, and 59.1×10^6 m^{-1}), respectively. The tests were run at the Vought Corporation wind tunnel in Dallas, Texas. The wind-tunnel model is shown in Fig. 3, with grooving of four grooves per inch (pitch = 0.25 in. or 6.35 mm). Both smooth and grooved models were tested. The results and test conditions for these cases are listed in Table 2.

III. Analysis and Correlations

A. Review of Existing Expressions

A quick review of existing expressions will be presented so that differences and similarities with the present work will be clarified.

Reference 2 provides an empirical relation in the form of

$$\Delta C_{D_g} = [0.00025 M^{3.9} l_g] C_{D_{TSB}} \tag{1}$$

where ΔC_{D_g} is the incremental drag coefficient due to grooves, based on the projectile reference area A_{ref} ($= \pi D^2/4$), where D is the reference diameter for the projectile.

Reference 3 provides the following expression for computing the incremental drag.

$$\Delta C_{D_g} = 1.6 \frac{l_g}{l_c} C_{D_{SFSB}} \tag{2a}$$

where

$$C_{D_{SFSB}} = (4 d_c l_c) c_f \tag{2b}$$

The skin-friction coefficient c_f is defined as

$$c_f = \frac{\tau}{0.5 \rho_\infty V^2 A_{ref}}$$

where τ is the skin-friction shear stress at the projectile surface.

Reference 3 did not specify the expression used for c_f in its application to the projectile configuration shown in Fig. 4. In this study, an expression for c_f for turbulent flow was used from Ref. 6 as

$$c_f = \frac{0.455(1 + 0.2 M_\infty^2)^{-0.32}}{(\log_{10} Re_L)^{2.58}} \tag{2c}$$

B. Present Analysis

The present approach is similar, in general, to the data-correlation approach used earlier in Ref. 7. The influencing

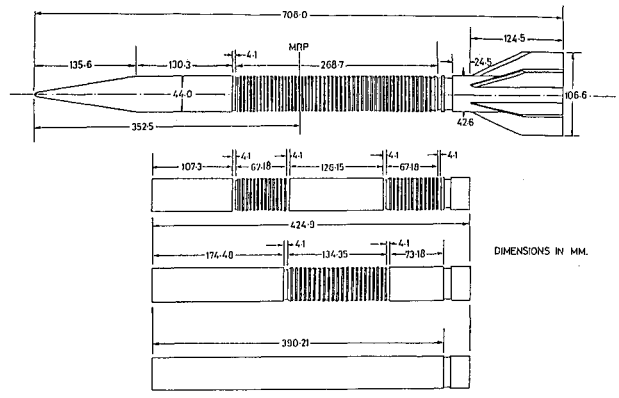

Fig. 4 Wind-tunnel test model for the tests of Ref. 3.

physical parameters are first identified, then some of the wind-tunnel data are used to determine the constants in the correlation. Finally, the rest of the data is used for validation of the obtained expressions.

First Expression

This expression is targeted only for "typical" KE projectiles as shown in Fig. 1. More specifically, the "typical" KE projectile is defined as one with nose-cone semivertex angle less than 9 deg, having a very small nose radius $\leq 0.03D$, with no boattail, and having one main cylindrical diameter. This expression is not valid for KE projectiles as shown in Fig. 3. The expression is formulated in the form of Eq. (1) (from Ref. 2), where the body-alone, smooth, total body drag coefficient is known, and only the incremental groove drag is required. This approach suits projectile designers where the groove drag is considered after all other design and shape requirements have been fulfilled.

First, considering the physical parameters that do affect the groove drag, one might write

$$\Delta C_{D_g} = F(M, Re, l_g, p, h, x_o)$$

where $p = 1/n$ and n is the number of grooves per unit length.

The parameter x_o was neglected based on the results of Ref. 3, which indicated no measurable effect on ΔC_{D_g} of slightly varying x_o. Also, the parameter h was eliminated since both p and h are directly related for all standard groove geometries. Therefore, the expression will be a function of the pitch p, which also can usually be more easily measured than h. The preceding expression is then simplified and written as

$$\Delta C_{D_g} = [F(M, Re, l_g, p)] C_{D_{TSB}}$$

Based on the data for the 17 cases of Ref. 1, the first correlation in the present work for typical projectiles is introduced as

$$\Delta C_{D_g} = \left[2.05 TF_1 \frac{l_g}{L} MF_1 RF_1 \right] C_{D_{TSB}} \tag{3a}$$

where TF_1 is the thread factor defined as

$$TF_1 = 0.84 + 0.117\left(\frac{p}{0.031}\right) - 0.007\left(\frac{p}{0.031}\right)^2 \tag{3b}$$

where p is the groove pitch in inches; MF_1 is the Mach number factor introduced as

$$MF_1 = \frac{1}{M_\infty^{(1.453 - 0.067 M_\infty)}} \tag{3c}$$

RF_1 is the Reynolds number factor introduced as

$$RF_1 = \left(\frac{4.2 \times 10^6}{Re}\right)^{0.8} \tag{3d}$$

and Re is the Reynolds number per foot.

For multiple grooves with different pitch on the same projectile, Eq. (3a) takes the form:

$$\Delta C_{D_g} = \left[2.05 \left(\frac{TF_{11} l_{g_1} + TF_{12} l_{g_2}}{L} \right) MF_1 RF_1 \right] C_{D_{TSB}} \quad (4)$$

where TF_{11} and TF_{12} are the thread factors for the threads of pitch p_1 and p_2, respectively.

One can notice the large differences between Eq. (3a) of this work and Eq. (1) of Ref. 2. The latter does not include Reynolds-number dependence or groove-pitch dependence. Furthermore, ΔC_{D_g} increases with the increase in Mach number, whereas in reality it decreases with Mach number. Also, Eq. (1) depends directly on l_g, whereas Eq. (3a) is found to be more appropriate if l_g/L is used.

Finally, Eq. (1) is found, as will be shown in the results, to give results as high as 10 times (1000%) the experimental value. Equation (3a) follows the data within $\pm 13\%$.

Second Expression

For nontypical KE projectiles, as shown in Fig. 3, it is not adequate to use $C_{D_{TSB}}$ as an input. This is because large variations in nose or boattail angles can cause large changes in $C_{D_{TSB}}$ even though the groove drag on the bodies will not change. Therefore, an approach like that of Ref. 3, which relates only to the cylindrical part of the projectile (i.e., excluding the nose and the boattail), should be more appropriate. Therefore, this expression is targeted to be more general than that of Eqs. (3).

Based on the data of Refs. 1 and 4, the second correlation for the general projectile configuration was found to have the form:

$$\Delta C_{D_g} = \left[2.59 TF_2 \frac{l_g}{l_c} MF_2 RF_2 \right] C_{D_{SFSB}} \quad (5a)$$

where

$$TF_2 = 1 + 0.1 \left(\frac{p}{0.031} \right)^a \quad (5b)$$

$$a = 0.528 \left(\frac{p}{0.031} \right)^{0.462}$$

$$MF_2 = M^{-[3.164 + 3.225 M^{0.4} - 0.156 M^{1.5}]} \quad (5c)$$

$$RF_2 = \left(\frac{9 \times 10^6}{Re_L} \right)^{0.6} \quad (5d)$$

and $C_{D_{SFSB}}$ is as given by Eq. (2b).

For configurations with multiple thread types, Eq. (5a) becomes

$$\Delta C_{D_g} = 2.59 \left(\frac{TF_{21} l_{g_1} + TF_{22} l_{g_2}}{l_c} \right) MF_2 RF_2 C_{D_{SFSB}} \quad (6)$$

Comparison of the present expression of Eq. (5) and that of Eq. (2) (i.e., from Ref. 3) reveals the following facts. First, the present analysis includes explicitly the effects of Mach number, groove pitch, and Reynolds number. None of these effects is considered by Ref. 3. Second, as will be shown, the results of applying the expression of Ref. 3, in general, overpredict the wind-tunnel data by 300%.

Since the second correlation expression [Eq. (5)] is more general, i.e., can be applied to all KE configurations (including the configuration of Fig. 3), it is recommended over the first correlation expression. However, in cases where both expressions apply, the results of those two expressions should be very close to each other.

IV. Results and Comparisons

Equation (3) (i.e., the first expression) was first applied to the configurations of Ref. 1. Seventeen cases were computed.

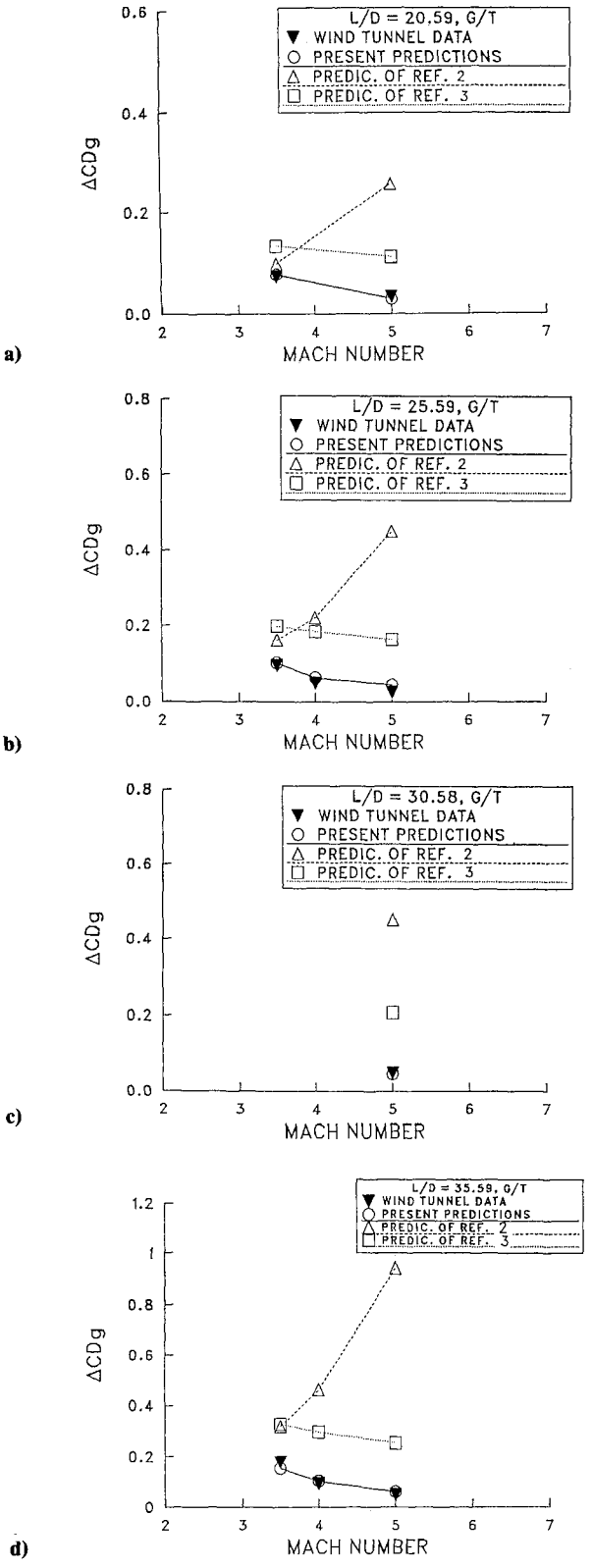

Fig. 5 Results of present correlation. Validation of ΔC_D with Mach number: a) for $L/D = 20.59$; b) for $L/D = 25.59$; c) for $L/D = 30.58$; and d) for $L/D = 35.59$.

Also, the expressions of Refs. 2 and 3 were applied and compared with the experimental data.

Figures 5a–5d show the variation of the incremental drag with the increase of Mach number for the four different L/D of 20, 25, 30, and 35, respectively. Figure 5a shows the predictions of Ref. 3 to be twice as high as the data, whereas those of Ref. 2 are much higher. Also, the trend given by Eq. (1)

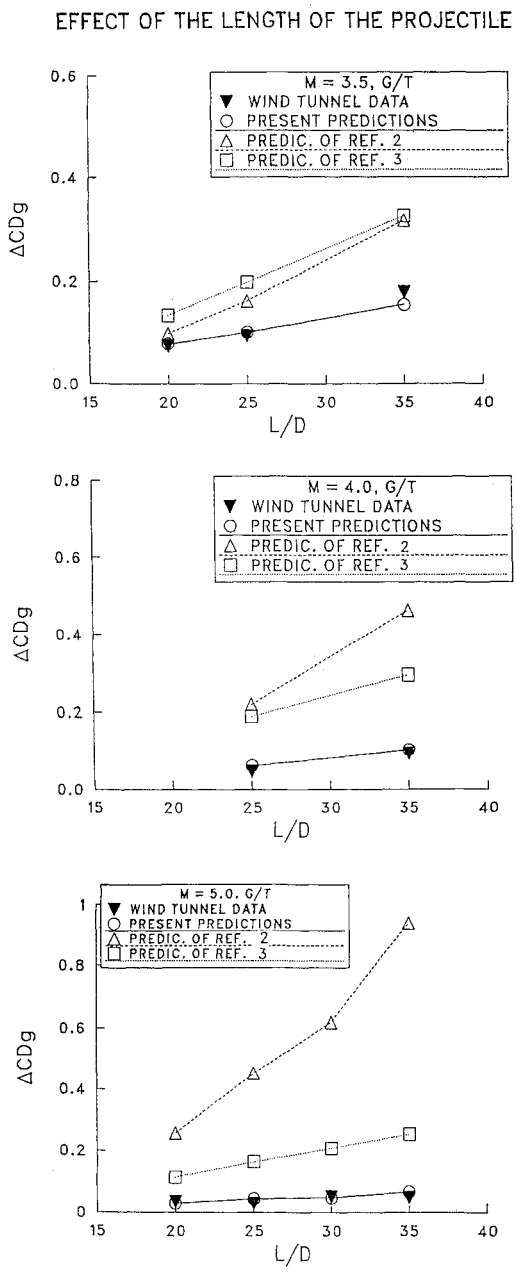

Fig. 6 Result of present correlation. Variation of ΔC_D with groove length l_g/D: a) $M = 3.5$; b) $M = 4.0$; and c) $M = 5.0$.

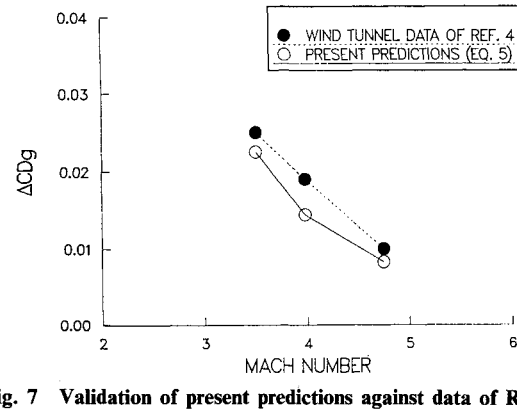

Fig. 7 Validation of present predictions against data of Ref. 4.

(from Ref. 2) is in the wrong direction compared to the data. Figures 5b–5d all show the same features as stated previously and also indicate the accuracy of the present correlation.

Figures 6a–6c show the effect of the length of the projectile (and hence the length of the grooved section) on the incremental drag, for each of the Mach numbers of 3.5, 4.0, and 5.0. The expressions of Refs. 2 and 3 overpredict the results by more than 100% as seen in Fig. 6a. The same results are repeated in Figs. 6b and 6c. In all of the cases, the present correlation predicts the results very accurately. It is of interest to notice that in Fig. 6c, Eq. (1) of Ref. 2 overpredicts ΔC_{D_g} by more than ten times for $L/D = 35$.

A summary of the present predictions of Eq. (3) and the wind-tunnel data of Refs. 1 and 4 is given in Table 3.

The second expression, Eq. (5), was applied to the test case of Ref. 4 where the first expression, Eq. (3), is not applicable. The results as shown in Fig. 7 are in good agreement considering the complexity of the shape. It is to be noted that the present results underpredict the data. This underprediction is expected since the grooves are known to increase the boattail drag.[8] This trend was shown in Ref. 8 where serrated body ends were tested in wind tunnels at subsonic speeds, causing an increase in the base drag. The effect of grooves on boattail drag is not included in this study; however, this effect explains why the present predictions for this projectile configuration must be smaller than those of the wind tunnel.

Table 3 Comparison of present predictions with data of Refs. 1 and 4

	C_D Wind tunnel		ΔC_{D_g}	
Case no.	Grooved body	Smooth body	Wind Tunnel	Present predictions Eq. (3)
1	0.213	0.197	0.016	0.0193
2	0.384	0.310	0.074	0.0779
3	0.231	0.197	0.034	0.0294
4	0.238	0.197	0.041	0.0331
5	0.256	0.236	0.020	0.0275
6	0.434	0.340	0.094	0.1005
7	0.328	0.280	0.048	0.0615
8	0.265	0.236	0.029	0.0429
9	0.277	0.236	0.041	0.0434
10	0.282	0.258	0.024	0.0312
11	0.308	0.258	0.050	0.0469
12	0.327	0.258	0.069	0.0509
13	0.298	0.248	0.050	0.0407
14	0.578	0.400	0.178	0.1532
15	0.450	0.357	0.093	0.1035
16	0.347	0.297	0.049	0.0603
17	0.354	0.298	0.056	0.0656
18	0.280	0.255	0.025	N/A[a]
19	0.227	0.208	0.019	N/A
20	0.196	0.186	0.010	N/A

[a]Not applicable.

Table 4 Comparison of the present two correlations

	ΔC_{D_g}		
Case no.	Wind tunnel	Present predictions Eq. (3)	Present predictions Eq. (5)
2	0.074	0.0779	0.0805
3	0.034	0.0294	0.0334
6	0.094	0.1005	0.1040
7	0.048	0.0615	0.0650
8	0.029	0.0429	0.0415
11	0.050	0.0469	0.0461
14	0.178	0.1532	0.1494
15	0.093	0.1035	0.0937
16	0.049	0.0603	0.0514
18	0.025	N/A[a]	0.0226
19	0.019	N/A	0.0144
20	0.010	N/A	0.0083

[a]Not applicable.

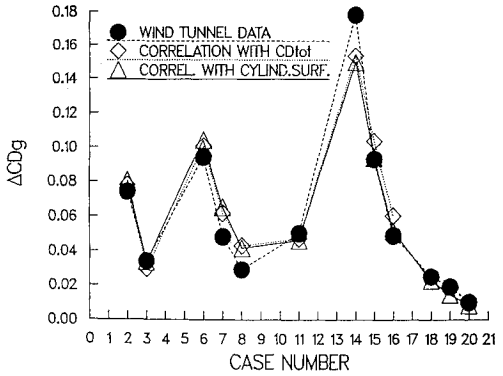

Fig. 8 Comparison of the results of the present two correlations.

The second expression, Eq. (5), was then applied to some of the cases of Ref. 1 to see how closely the two correlation expressions compare. Nine of the seventeen cases were recomputed and the results were very similar. Those results and a comparison with the earlier results of the first expression, Eq. (3), are given in Table 4.

A summary plot for the comparison of the present two prediction correlations, Eqs. (3) and (5), with the wind-tunnel data is given by Fig. 8. The predictions are shown to be in good agreement with the data.

It is felt that the most influential factor is the Reynolds number, followed by the Mach number. The incremental groove drag decreases significantly with an increase in Reynolds number. It also increases rapidly with the decrease of Mach number towards the sonic value. The present correlations are only to be used for $M \geq 3.5$, since the Mach number function was targeted for that region only. It is found that for $M < 3.5$, the Mach number function may greatly overpredict the expected answer.

V. Summary and Conclusions

A fast prediction capability for computing the incremental drag of kinetic energy projectiles due to surface grooves at supersonic speeds has been established. Physical variables affecting the groove drag have been identified and studied with respect to their importance.

Two correlations with wind-tunnel data are established for typical and general KE projectile configurations. The second correlation is recommended since it can be applied to many KE projectile configurations. The correlation expressions are valid only for the Mach range $3.5 \leq M < 5.5$ and for $\alpha = 0$ deg. Any application for Mach numbers less than 3.5 will yield overpredicted results.

Comparison with other existing prediction expressions heavily favored the present correlations. The accuracy of these present correlations is $\pm 20\%$, whereas the existing prediction methods of Refs. 2 and 3 can be as high as $+1000\%$ and $+300\%$, respectively.

Finally, the Reynolds number is expected to play a significant role. The incremental drag decreases significantly with the increase of Reynolds number. It is hoped that more tests will be available at the Reynolds number of $35 \times 10^6\ \text{ft}^{-1}$ rather than the present values of $4\text{–}6 \times 10^6\ \text{ft}^{-1}$. These tests could be run in cryogenic wind tunnels and the results further be used to validate the present correlations.

References

[1]Brandon, F. and Von Wahlde, R., "Wind-Tunnel Data for Long-Rod Fin-Stabilized Projectiles," U.S. Army Ballistic Research Lab., Aberdeen Proving Ground, Md, BRL-MR-3618, July 1987.

[2]Donovan, W. F., Nusca, M. J., and Woods, S., "Automatic Plotting Routines for Estimating Static Aerodynamic Properties of Long-Rod Finned Projectiles for $2 < M < 5$, U.S. Army Ballistic Research Lab., Aberdeen Proving Ground, Md, ARBRL-MR-03123, Aug. 1981.

[3]Hendry, C. E., "Contract MW 22B/807—Aerodynamics of Long Projectiles—Final Report, Part 2," British Aerospace PLC, Dynamics Group, Sowerby Research Centre, Bristol, England, UK, Rept. JS 10134, Aug. 1984.

[4]Meissner, R. and Malinoski, F., Unpublished wind-tunnel data, U.S. Army Ballistic Research Lab. Aberdeen Proving Ground, Md, Aug. 1987.

[5]Mikhail, A. G., "Data Correlation and Predictions of Surface Groove Drag for Kinetic Energy Projectiles," AIAA Paper 88-2541, June 1988.

[6]McCoy, R. L., "McDRAG"—A Computer Program for Estimating the Drag Coefficient of Projectiles," U.S. Army Ballistic Research Lab., Aberdeen Proving Ground, Md, ARBRL-TR-02293, Feb. 1981.

[7]Mikhail, A. G., "Fin Gaps and Body Slots: Effects and Modeling for Guided Projectiles," U.S. Army Ballistic Research Lab., Aberdeen Proving Ground, Md, BRL-TR-2808, June 1987. (Also, *Journal of Spacecraft and Rockets,* Vol. 25, Sept.-Oct. 1988, pp. 345–352; also AIAA Paper 87-0447, Jan. 1987.)

[8]Gai, ɔ. L. and Patil, S. R., "Subsonic Axisymmetric Base Flow Experiments with Base Modifications," *Journal of Spacecraft and Rockets*, Vol. 17, Jan.–Feb. 1980, pp. 42–46.